Int J Adv Manuf Technol (2017) 91:1–11
DOI 10.1007/s00170-016-9713-y

ORIGINAL ARTICLE

Numerical and experimental investigations on large-diameter gear rolling with local induction heating process

Xiaobin Fu[1] · Baoyu Wang[1] · Xiaoxing Zhu[1] · Xuefeng Tang[1] · Hongchao Ji[1]

Received: 30 April 2016 / Accepted: 7 November 2016 / Published online: 15 November 2016

Abstract Gear rolling with local induction heating process is a novel method to produce large-diameter gears with great advantages. To investigate the gear forming process, a simplified finite element (FE) model coupling electromagnetic-thermal and deformation fields is developed in the DEFORM-3D software and is validated by corresponding experiments. According to the numerical and experimental results, producing large-diameter gears using gear rolling process with local induction heating is feasible. Moreover, the blank heated by local induction heating has a temperature gradient distribution in the radial direction, which results in the defect reduction of inner hole enlarging. Thanks to the heat compensation function of induction heater, the defect of metal folding in the tooth top of the blank is reduced. In addition, the formability is improved by using local induction heating and the rolling force drops drastically compared with cold rolling process.

Keywords Gear rolling · Local induction heating · Finite element modeling · Experiment

1 Introduction

Involute gears are essential machine parts in many types of devices, especially in the transportation equipment. Gears are applied to transferring power with a certain ratio of palstance between two shafts. In addition, they are applied to transmitting a particular angular motion from one shaft to another. In both cases, they usually suffered cyclic load and severe stress. [1] The majority of gears are machined from blanks by hobbing followed by a finishing process. These processes are technologically demanding, and they produce a lot chips as waste. As a result, there is industry interest in the near net shape forming of gears, which is becoming increasingly important due to a potential high degree of material utilization.

In recent years, many research efforts have been conducted to analyze metal forming processes for gear production. Dean et al. [2, 3] studied the forming of bevel gears and helical gears by forging and designed a completely closed cavity toolset, which is capable of reducing forging loads and improving accuracy of the produced gears. According to the results of the fatigue tests carried out, they concluded that there is a great improvement of the fatigue limit of forged gears compared with that of cut gears. Choi et al. [4] employed an upper-bound analysis to investigate the spur gear forging process and found that to reduce the forging load, using a hollow billet instead of a solid one was more effective. Moreover, the suitable number of teeth for the forging of a spur gear was recommended to be between 15 and 20, which reveals that the gear forging process is suitable for the gears with minor modules and diameters. Wang et al. [5] investigated the deformation of spline gear parts using a two-step warm extrusion process and analyzed the influence of the lubrication condition and entrance angle on the deformation. Li et al. [6] proposed ironing finishing and compressing finishing methods to improve the accuracy of the hot-forged helical gears and compared the finishing loads and surface roughness between the two finishing methods.

The cross rolling technique applied to forming the involute tooth-like parts, such as involute spline shafts, was developed

✉ Baoyu Wang
bywang@ustb.edu.cn

Xiaobin Fu
fu_george@sina.com

[1] School of Mechanical Engineering, University of Science and Technology Beijing, No. 30 Xueyuan Road, Haidian District, Beijing 100083, China

by Anderson Cook Corporation in the 1950s and was entered into practical use in the 1970s. Egan et al. [7] outlined the interrelationship of warm and hot rolling to cold rolling and the limitations on the cold rolling. Kamouneh et al. [8, 9] investigated the effects of the machined method on the strength of the gear tooth and got a conclusion that compared with traditionally machined parts, flat-rolled gears had a 50% improvement in hardness and a higher fatigue limit through metallurgical examination together with validation and simulation results. Neugebauer et al. [10–12] described an unconventional pitch design of gear dies and noted that compared with rack dies, round dies need extra kinematic compensation during rolling process. With the compensation considered, the pitch error of the formed gear was improved by 50%, which makes it possible to form the high teeth gears (up to 10 mm in height and a tooth height coefficient larger than 2.7) by cross rolling. Zhang et al. [13] proposed the thread and spline synchronous rolling process, which realized the synchronous deformation of the external thread and external spline tooth profile. Moreover, the phase characteristic between dies before rolling for thread and spline synchronous rolling process was investigated. [14] Li et al. [15] analyzed the slippage phenomenon during the cold gear rolling process using numerical and experimental methods.

The aforementioned previous studies mainly focused on producing minor-diameter gear parts or spline shafts. However, the deformation of large-diameter gear parts by near-net shaping is rarely studied because of high forming loads, which results in short tool life and high equipment requests. In this paper, to produce large-diameter gear parts, the gear rolling process with induction heating was applied. The rolling machine was redesigned to meet the forming requirement. A simplified model coupled with the electromagnetic thermal and deformation fields was established. The experiment of gear rolling with induction heating was carried out. According to the simulation and experimental results, the temperature distribution, metal flow, and improved formability due to the local induction heating process were analyzed.

2 Process principle

The principle of the gear rolling with local induction heating process is shown in Fig. 1. The process includes the following steps. First, the clamper clamps the blank firmly and the rotating devices drive the blank to rotate. Simultaneously, the inductor heats the outer layer of the blank. When the temperature of the blank reached a pre-set value, the gear die is rotated and pushed to approach the blank by the feeding device. Then, the blank is forced to form the teeth gradually. Once the gear die is pushed to reach the designated position, the feeding device stops, while the blank and the die continue rotating. Finally, the blank and the die rotate in the opposite direction to finish the formed teeth.

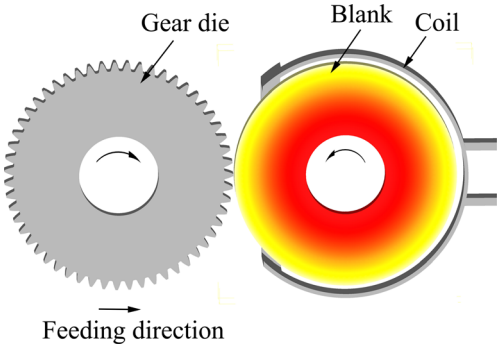

Fig. 1 The principle of gear rolling process with local induction heating

3 Model establishment

3.1 Material model

SAE 8620H is a low-carbon alloy steel used in manufacturing gear parts. Owing to the addition of nickel and molybdenum, its hardenability, distortion of heating treatment, and high temperature performance are improved. Therefore, the application of SAE 8620H is now extended to manufacturing large-diameter gear parts. Table 1 shows the chemical composition of SAE 8620H. To establish the constitutive model used in the finite element (FE) model, the flow stress of SAE 8620H gear steel was obtained by an isothermal compression test at 1223–1373 K with a strain rate of 0.1–10 s^{-1}, using a Gleeble-1500D thermosimulation machine. Figure 2 shows the flow stress–strain curves under different deformation conditions. The flow stress–strain curves are fitted to a formula according to the Arrhenius equation [16, 17] as follows:

$$\dot{\varepsilon} = A[\sinh(\alpha\sigma)^n]\exp\left(\frac{-Q}{RT}\right) \quad (1)$$

where $\dot{\varepsilon}$ is the strain rate, A and α are the material constants, and η is the inversely identical exponent of strain rate sensitivity. Q is the activation energy for deformation, R is the gas constant, and T is the temperature. Table 2 shows the calculated material parameters. In this model, the hardening rule is isotropic and the yield criterion follows the von Mises yield criterion.

Table 1 Chemical composition of SAE 8620H gear steel (wt%)

C	Cr	Ni	Mo	Mn	Si	Cu	S	P	Al	Fe
0.20	0.57	0.46	0.20	0.85	0.25	0.09	0.003	0.011	0.02	Bal.

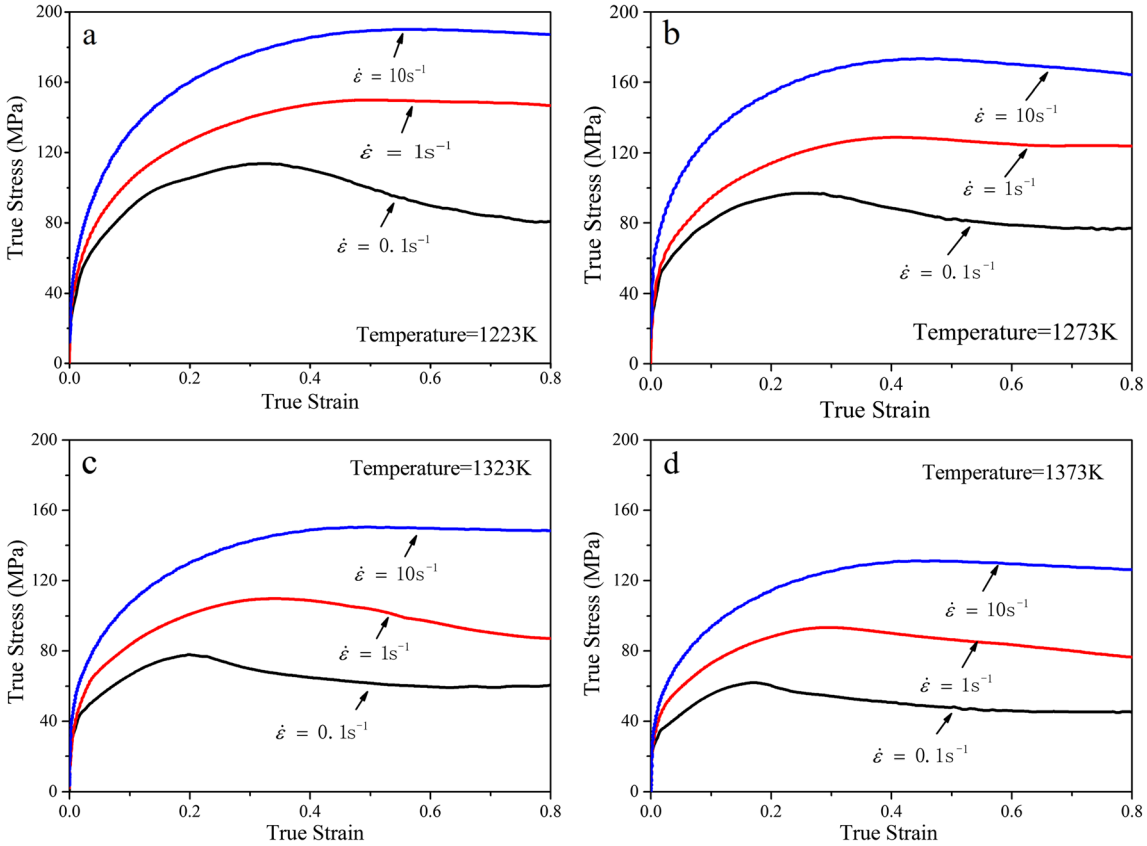

Fig. 2 True stress–strain curves for SAE 8620H alloy steel under different deformation conditions: **a** 1223, **b** 1273, **c** 1323, and **d** 1373 K

The material model described by the Arrhenius equation was set in the DEFORM-3D preprocessor and loaded on the element of the gear blank.

3.2 FE model

3.2.1 FE model of induction heating

As shown in Fig. 1, the shape of the coil is circle with a gap to allow the gear die to squeeze the blank. During the heating process, the blank is rotated, and the effects of the coil gap on the electromagnetic and thermal fields can be ignored. The heating model can be simplified and assumed to be axisymmetric. The simplified FE model of the induction heating is developed in the COMSOL Multiphysics software, as is shown in Fig. 3. The model includes the blank, the coil, and the air. Carrying high-frequency current, the coil generates an alternating magnetic field, which in turn induces eddy currents in the blank that dissipate energy and bring about heating.

Table 2 Calculated parameters of material from constitutive model

Parameter	A (s^{-1})	α (MPa^{-1})	n	R (J/mol/K)	Q (kJ/mol)
Value	3.2×10^{12}	8.8×10^{-3}	4.816	8.314	318.94

Table 3 shows the material and shape parameters used in the simulations. The relationships of the electromagnetic and thermal properties with temperature of SAE 8620H alloy steel [18] are illustrated in Fig. 4. In this model, the ambient temperature is set as 293 K and the convection heat transfer coefficient with air is 2000 W/(m^2 K).

The mesh of the simplified axisymmetric model is shown in Fig. 5. A tetrahedral mesh is generated in the model, and the number of the elements is 20,000. Considering the skin effect, the eddy current is large in the outer layer of the blank. The mesh of the blank is locally refined, and the length of the elements in the outer layer of the blank is set as 1 mm.

In the COMSOL Multiphysics software, the electromagnetic field (EMF) module and the heat transfer (HT) in solid

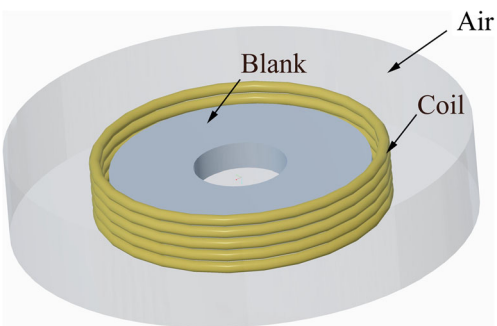

Fig. 3 The simplified physical model of induction heating

Table 3 Materials and shape parameters used in the simulation

Blank				Coil			
Material	Outside diameter	Inside diameter	Height	Material	Caliber	Diameter	Thickness
SAE 8620H	280 mm	100 mm	30 mm	Copper	8 mm	150 mm	1 mm

module are applied to the calculation of the heating process. In the EMF, the electromagnetic heat is calculated, and the results are sent to the HT module to calculate the temperature distribution in the blank. The temperature data are shared with the EMF module. According to the temperature data, the temperature-related parameters are updated and applied to calculating the EMF in the next step. The flowchart of the coupled electro-magneto-thermal analysis is shown in Fig. 6.

After the calculation of the heating process is performed, the temperature distributions, heating rates, and heating sources can be exported.

3.2.2 FE model of gear rolling process

The model of the gear rolling process is established in the DEFORM-3D software and composed of the blank, gear die, and two baffles, as shown in Fig. 7a. The blank is heated by induction heating, and the two baffles are mounted on both ends of the gear die to prevent the metal of the blank from flowing along axis direction. During the process of deformation, the blank and gear die rotated along their own axes, while their rotational velocities were in opposite directions. At the same time, the gear die approached the blank gradually. Finally, the blank was squeezed and the teeth were formed at the outer layer.

As the gear parts are symmetrical and the rolling force is periodical, to save the computing time and storage [13, 19], 1/24 of the blank is chosen to be the model and is assumed to be a plasticity body which is fixed, as shown in Fig. 7b. The gear die and baffle plate, which are set as rigid bodies, revolved on their own axis and the axis of the blank at the same speed of 1.5 rad/s. The feeding speed of the gear die is set as 0.2 mm/s. The friction coefficient between the gear die and blank is assumed to be constant during the whole rolling process. The frictional force in the shear friction model is defined as follows:

$$fs = m \times k \tag{2}$$

where fs is the frictional stress, k is the shear yield stress, and m is the friction factor [20]. The fraction factor between the blank and gear die is 0.3.

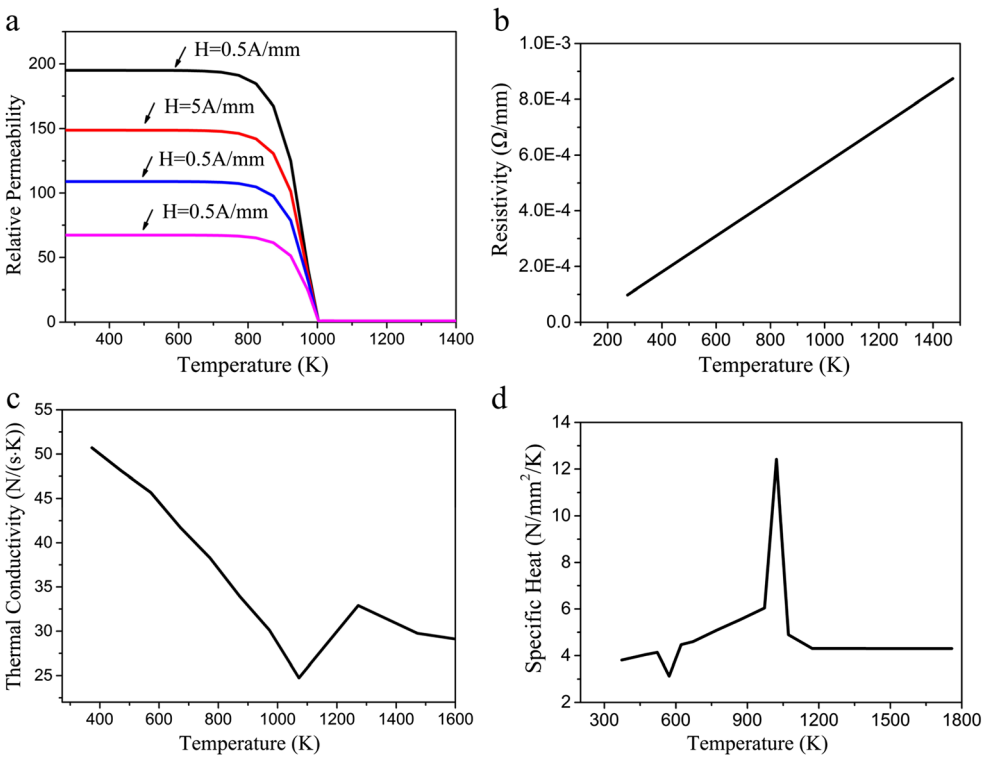

Fig. 4 The relationship of thermal and electromagnetic properties with temperature for SAE 8620H steel. **a** Relative permeability, **b** resistivity, **c** thermal conductivity, and **d** specific heat

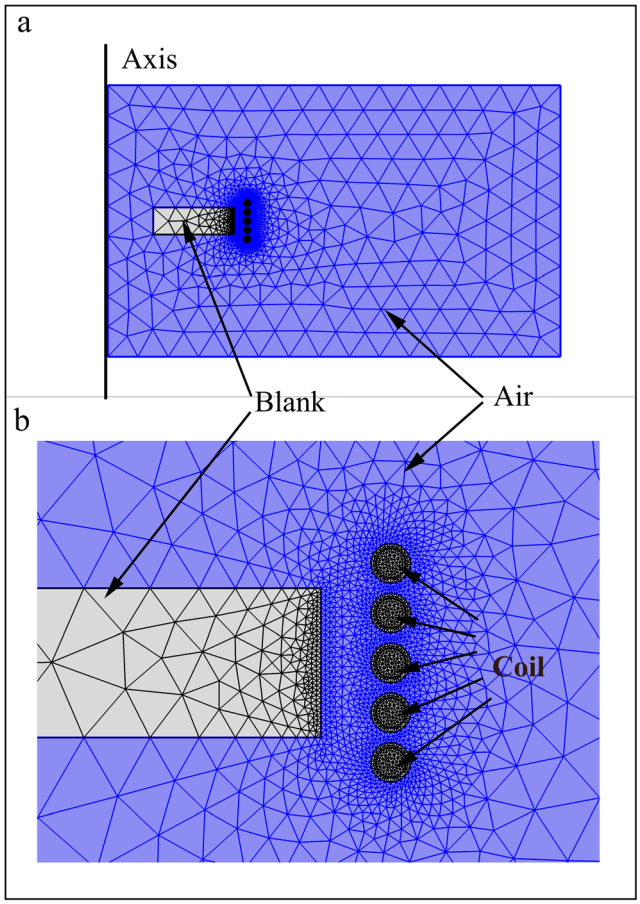

Fig. 5 **a** The FE mesh of the whole model and **b** the FE mesh of coil and blank

Since the deformation zone is mainly distributed in the outer layer, the mesh in the deformation zone is refined and the ratio of refinement is 0.01. The FE mesh of the blank is illustrated by Fig. 7c.

During the rolling process, owing to the contact with the cold die, the temperature of the outer layer of the blank drops. To obtain good plasticity to make the blank easily deformed, the heat compensation program is employed. If the infrared sensor detects that the temperature is lower than the pre-set value, the induction heater is commanded on, and if the temperature is higher than the pre-set value, the induction heater is set to shut off to stop heating. To simulate the heat compensating program, the DEFORM-3D software is secondarily developed. If the highest node temperature is lower than the pre-set value, the distribution of the electromagnetic heat is going to be set as the heat source boundary condition to simulate the heat compensating process. If the highest node temperature was higher than the pre-set value, the heat source of all nodes was set to be zero. Ignoring the radial dimension changes of the blank, the relationship of the electromagnetic heat with the coordinate is fitted and given as follows:

$$\begin{cases} f(r,z) = \dfrac{p_1 - p_2(R-r) + p_3 z}{1 + p_4(R-r) - p_5 z + p_6 z^2 - p_7 z^3} \\ r = \sqrt{x^2 + y^2} \end{cases} \tag{3}$$

where x, y, and z are the coordinates and R is the radius of the blank. $p_1 - p_7$ are the factors solved by curve fitting. The values of the factors are shown in Table 4. The R^2 value is 0.964.

4 Experiment of gear rolling process by local induction heating

The system of gear rolling by local induction heating is shown in Fig. 8. During the process, a high-frequency induction heating power supply and transformer provided high-frequency harmonic current to the inductor. Three servo motors were applied, two of those were used to provide the rotational power to drive the gear die and blank to rotate at a speed of 14.33 r/min. The other one was used to provide the feeding power to drive the gear die to approach the blank at a speed of 0.2 mm/s.

The roll forming force was measured by a pressure sensor. The temperature values were measured by infrared thermometer, while the current and the frequency values were measured by a multimeter.

5 Results and discussions

5.1 Experimental results

5.1.1 Inner hole enlargement during the rolling process

During the gear rolling process, the inner hole is suffering radial rolling force. As it is a datum during the tooth forming process, the distortion of the inner hole may result in imprecise teeth profiles. Thus, it is of importance to minimize the distortion of inner hole. In addition, increasing the temperature of the forming zone (the outer layer of the blank) can reduce the deformation resistance, resulting in a decrease of the rolling force.

To heat the forming zone, a local induction heating method and heating in a furnace are employed. The experimental results of the inner hole enlargement tests using two heating methods are shown in Table 5. Compared with the heat method in the heating furnace, the local induction heating method reduces the defect of the inner hole enlargement by approximately 95%. This effect occurs because when using the local induction heating method, there is a radial gradient. The lowest temperature is located at the inner hole, and the highest temperature is located at the forming zone, which results in a decrease of deformation resistance at the forming zone with

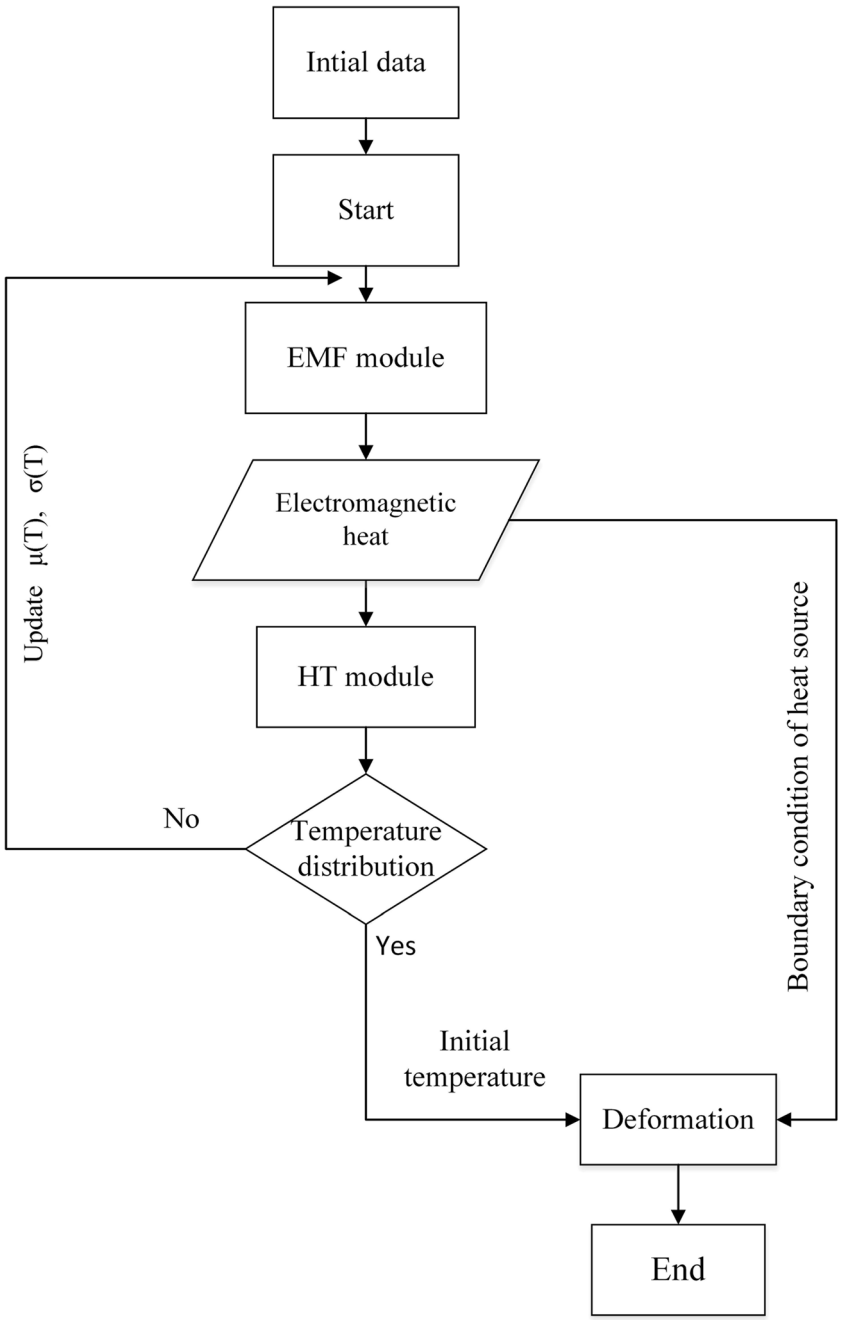

Fig. 6 Flowchart of the coupling process

the premise of nearly unchanged deformation resistance at the inner hole. While in the case of heating in a furnace, the blank has a uniform temperature distribution, resulting in the deformation resistance decreasing in the entire blank. Consequently, the inner hole is easily enlarged.

5.1.2 Metal folding in the tooth top

During the rolling process while heating in a furnace, the blank is heated uniformly, and due to the contact with the cold die, the temperature of the deform zone drops. With relatively low temperature near the tooth top, the metal is not likely to flow along the tooth profile radially, which likely leads to the defect of metal folding in the tooth top occurring, as Fig. 9a shows. Compared with the heating method in a heating furnace, owing to the heat compensating function of the induction heater, the outer layer of the blank remains at the same temperature, which means that during the tooth forming process, the metal near the tooth top flows easily along the tooth profile, radially. As a result, the tooth top can be well formed using the local induction heating, as shown in Fig. 9b.

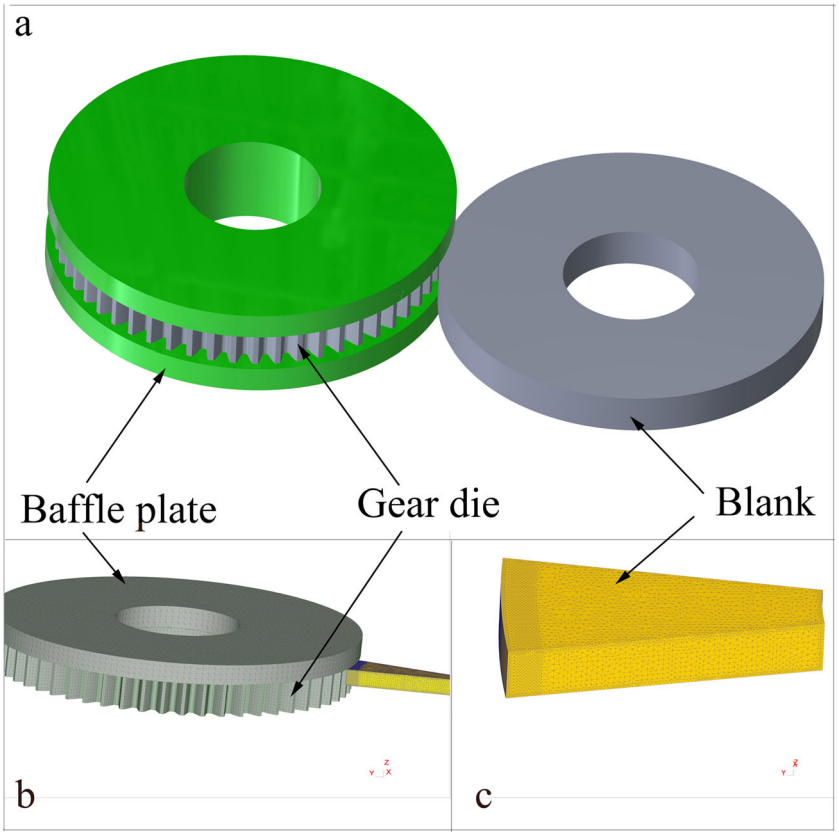

Fig. 7 Physical and FE models of gear rolling process. **a** The physical model, **b** the simplified FE model, and **c** the FE mesh of the blank

5.2 FE simulation results

5.2.1 Heating rate and temperature field

A point located in the middle of the outer wall of the blank is chosen to investigate the heating rate. The heating rate during the process is shown in Fig. 10. The duration of the temperature rising from 293 K (ambient temperature) to 1003 K (Curie temperature) is approximately 20 s. When the temperature is beyond 1003 K, the heating rate decreases significantly because when the temperature is beyond the Curie point, the relative permeability of the ferromagnetic material is going to change to be 1 suddenly. As a result, the magnetic flux density and the electromagnetic heating power decrease. Additionally, with the increase in the temperature of the blank, the heat dissipation by the convection from the surface of the blank to the air as well as radiation to the environment increases, which results in the decrease of the heating rate.

The axial (thickness direction) and radial temperature distributions before the rolling process are shown in Fig. 11.

Table 4 Parameters of the formula of the electromagnetic heat distribution

Parameter	p_1	p_2	p_3	p_4	p_5	p_6	p_7
Value	0.7465	−0.251	0.023	2.421	−0.134	0.049	−0.003

Figure 11a shows that the axial distribution of the temperature is not uniform in the outer layer. The lowest temperature is located in the middle of the thickness, and upon an increase in the distance in the axial direction, the temperature rises. At the edges, the temperature is the highest, which is related directly to the distortion of the EMF in those areas. This phenomenon is caused by the applied current frequency, relative coil blank height, and current intensity. Three different points belonging to three curves respectively at the same height axially are selected to compare. When the distance between the outer layer increases, the temperature

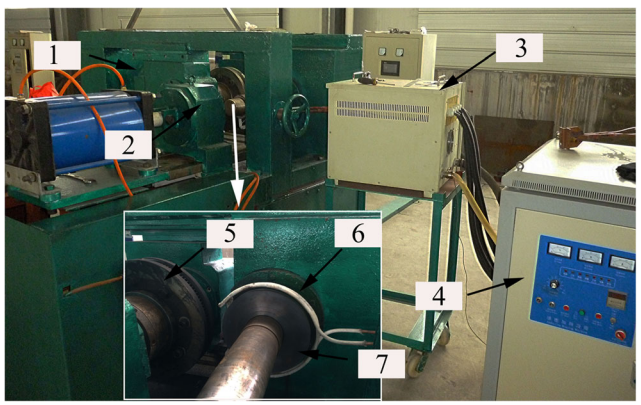

Fig. 8 The system of gear rolling with local induction heating. *1* Feeding device, *2* clamper, *3* transformer, *4* power supply of induction heating and *5* gear die and baffles, *6* coil, and *7* blank

Table 5 Comparison of the inner hole enlargement using different heating methods

Item	Enlarging value (local induction heating) (mm)	Enlarging value (heating in furnace) (mm)
1	0.16	3.45
2	0.14	3.62
3	0.17	3.48
4	0.15	2.91

of the point decreases, which indicates that the temperature distribution in the radial direction has a gradient, which is shown in Fig. 11b in detail.

5.2.2 Effective stress and effective strain analysis

Figure 12 shows the contour of effective stress during different stages of the gear rolling process. As Fig. 12a shows, during the penetration stage, the maximum effective stress emerges near the contact position between the blank and the gear die. Away from the contact position, the effective stress decreases. During the forming stage shown in Fig. 12b, the maximum effective stress increases compared with that in the penetration stage. Moreover, the area where the effective stress is beyond 50 MPa expands along the radial direction. With the feeding motion, the penetration of the gear die becomes deeper; thus, the contact area becomes large compared with that of the area in the penetration stage, leading to an increase of the effective stress and the expansion of the high effective stress area in the axial direction. During the finishing stage, the maximum effective stress emerges in the root of the formed tooth. After the teeth have been formed and the feeding motion has been finished, the area with high effective stress shrinks along the radial direction.

Figure 13 shows the contour of the effective strain during the gear rolling process in different stages. During the penetration stage, since the outer layer of the blank is squeezed by the teeth of the gear die, the maximum effective strain emerges

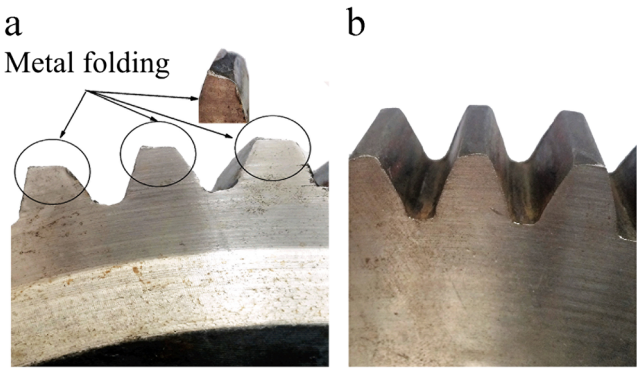

Fig. 9 Formed gears using different heating methods. **a** Heating in the furnace and **b** local induction heating method

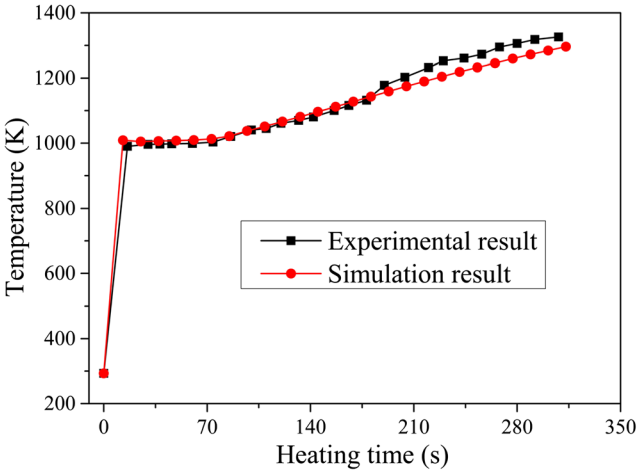

Fig. 10 Relationship of the temperature of the specific point with heating time shown in simulation and experimental results

at the indentation of the blank, as Fig. 13a shows. During the forming stage, as the teeth of gear die penetrate deeper, the area with high effective strain expands along the tooth profile,

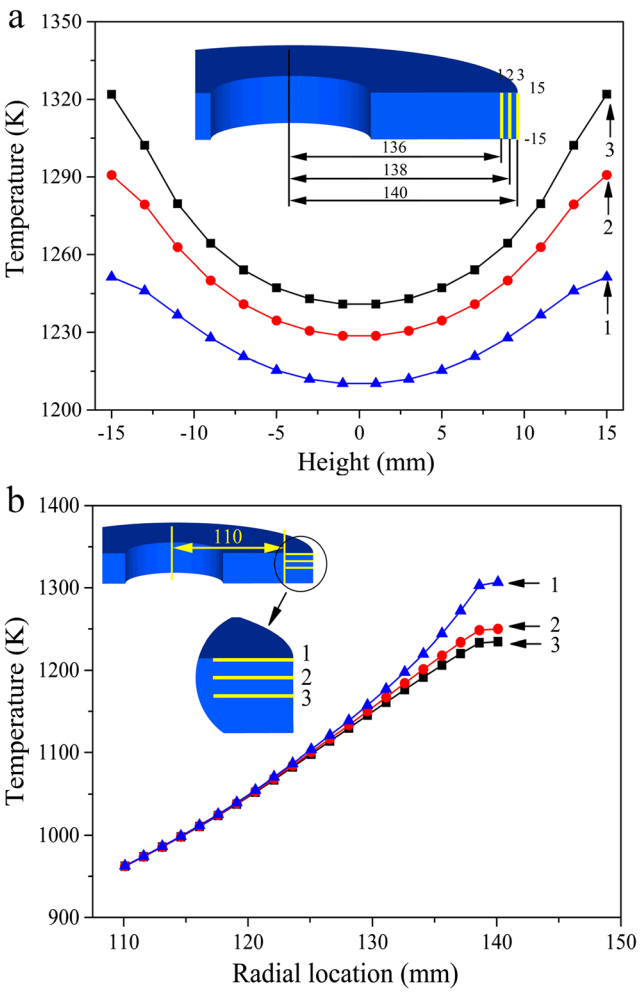

Fig. 11 Axial and radial temperature distributions in the outer layer of the blank. **a** Axial direction and **b** radial direction

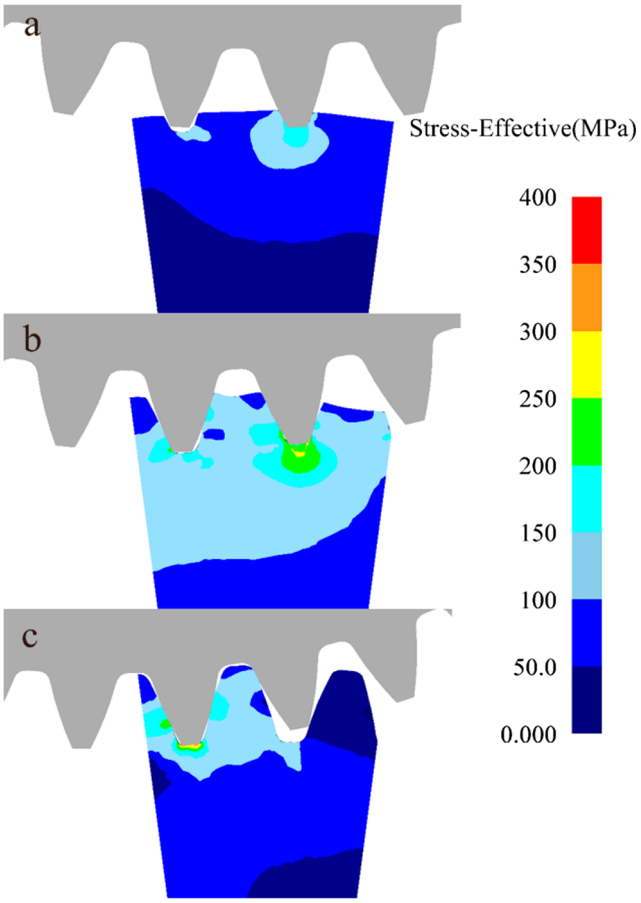

Fig. 12 The contour of effective stress during the gear rolling process. **a** Penetration stage, **b** forming stage, and **c** finishing stage

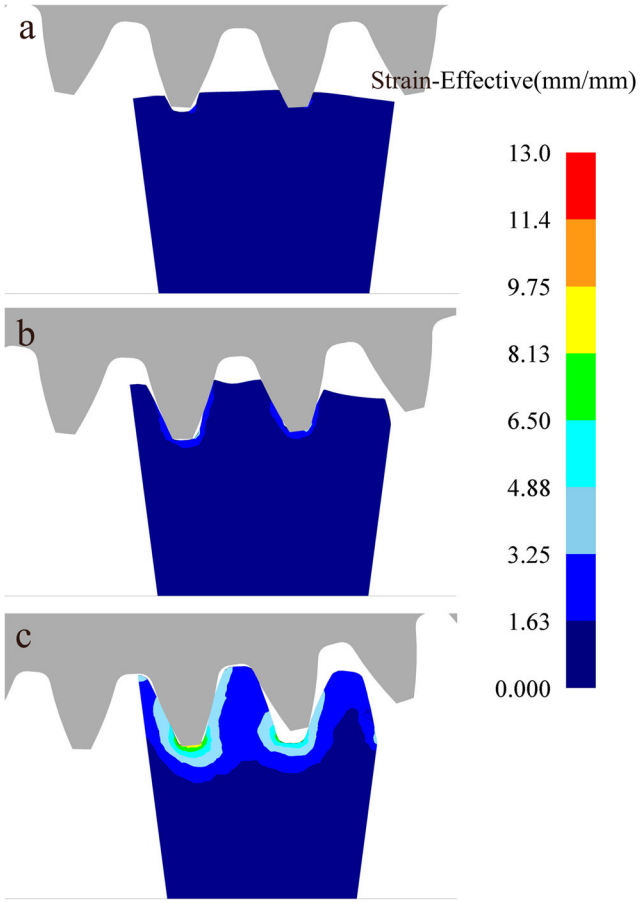

Fig. 13 The contour of effective strain during the gear rolling process. **a** Penetration stage, **b** forming stage, and **c** finishing stage

compared with that in penetration stage. During the finishing stage, the maximum effective strain emerges in the root of the formed teeth. Along the tooth profile, the effective strain is high compared with that in the top of the formed teeth. In addition, the effective strains at the left and right profiles are different, which indicates the difference of the metal flow between left and right tooth profiles.

5.2.3 Metal flow

During the rolling process, under squeezing by the rotating gear die, the metal of the blank flows. To study the metal flow, a flownet is employed in the DEFORM-3D postprocessor as a series of uniformly distributed concentric circles, as shown in Fig. 14a. Figure 14 shows the flownet of the blank in different stages. As the flownet of concentric circles changes, some concave–convex distortions occur on different levels. The rate of distortion at the edge of the blank is the greatest, and as the radius of the blank decreases, the rate of distortion decreases. The flownet at the edge has changed into the tooth shape, and away from edge, in the radial direction, almost no distortion is observed and it keeps its original shape. This result means that the major deformation zone is distributed in a certain depth of the outer layer.

According to the principles of metal forming, during plastic forming, metal is always going to flow along the direction of least resistance. From simulation results, the direction of the metal flow could be inferred from the direction of the concave–convex distortions of the flownet. In the tooth root of the blank, the flownet has a concave distortion, and as the intervals of the adjacent flownet decrease at the top of the tooth, a convex distortion appeared. However, the intervals of the adjacent flownet increase. Moreover, the intervals become larger as they near the outer layer. Because during the rolling process, the metal in the tooth root is squeezed by the gear die and flows to the inside radially, which results in densification of the metal in the tooth root. The degree of the density of the metal in the tooth root is very limited because the blank is supposed to have a constant volume during the plastic forming process. At the tooth top of the gear die, the metal of the blank does not suffer any pressure. As a result, instead of flowing to the inside radially, the metal near the tooth root flows along the tooth profile of the gear die towards the tooth top of the blank, and a convex flownet appears. With increasing the feeding, the rate of the

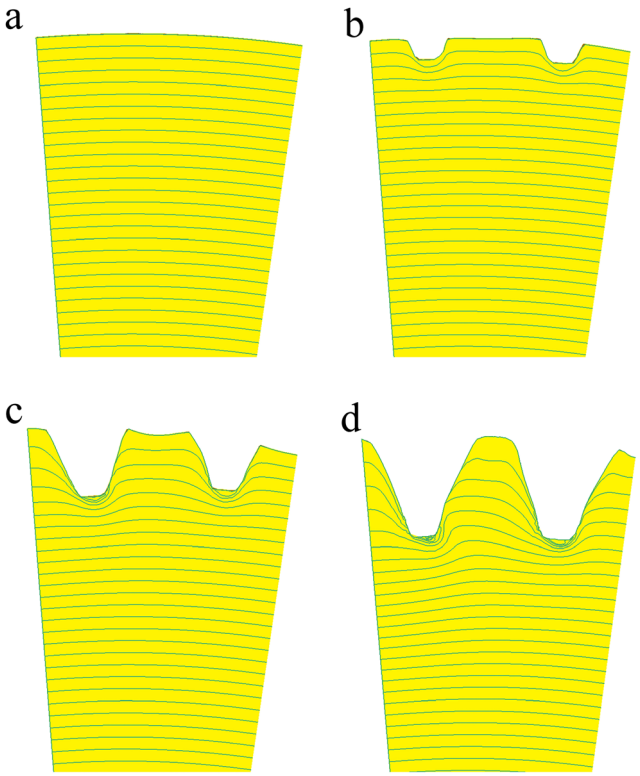

Fig. 14 The flownets of the blank during the following stages: **a** initial, **b** penetration stage, **c** forming stage, and **d** finishing stage

convex flownet gets larger, and finally, the tooth root of the gear is filled with the metal of the blank. Then, the tooth top of the blank is formed.

5.2.4 Rolling force

With the local induction heating process, the blank is heated and has a radial gradient temperature distribution. Owing to a high temperature in the forming zone, the yield strength of the material decreases and results in a decrease of the rolling force. Figure 15 shows the simulation and experimental results of the rolling force with time during different stages. From the figure, with a gradual increase of the feeding distance, the rolling force increases, and in the finishing stage, the rolling force drops and keeps a relatively constant value. During the gear die withdrawing stage, the gear die withdrew while suffering severe fraction force from the baffles, and as the withdraw distance increases, the rolling force decreases to zero. Moreover, the comparison between simulation and experimental results was carried out and the maximum relative error is 13.7%, which indicates that the simulation results match well with the experimental data and the FE model is considered verified. Therefore, the simulation results of the cold rolling force are also reliable. As Fig. 16 shows, the simulation rolling forces of cold rolling and rolling with local induction heating during the penetration and forming stage were extracted and compared with the maximum cold rolling force of 704 kN. The one with local induction heating is approximately 161 kN, a drastic reduction of 77%, which could improve the formability and minimize device requirements.

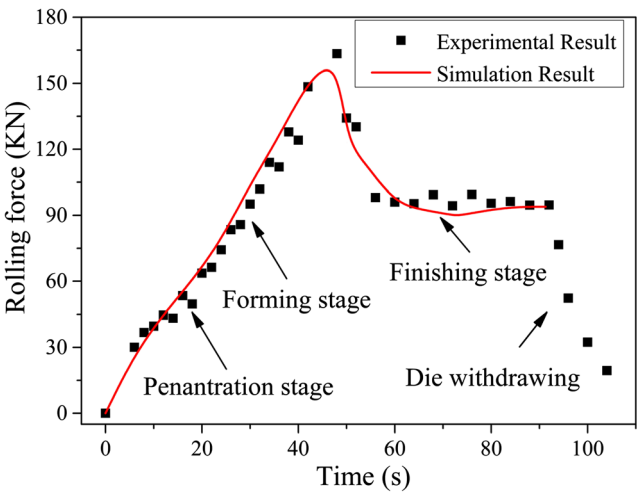

Fig. 15 Simulation and experimental results of rolling force during different stages

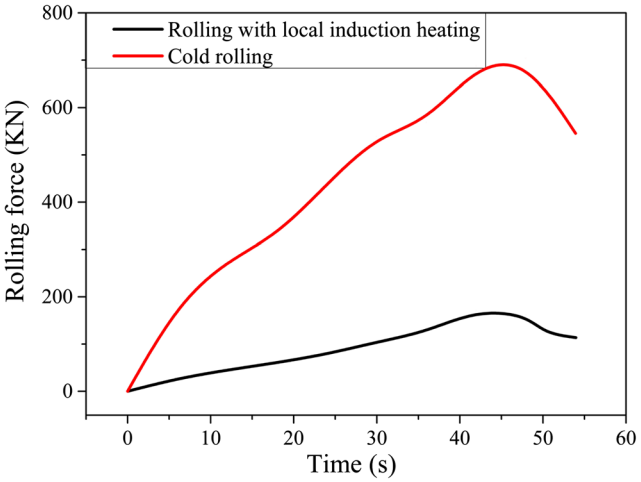

Fig. 16 Comparison of rolling force with different heating methods during the penetration and forming stage

6 Conclusions

To form large-diameter gears with a large module, the local induction heating process was employed. A simplified FE model coupling electromagnetic, thermal, and deformation fields was developed in DEFORM-3D to simulate the gear rolling process using local induction heating. Gear rolling experiments were conducted. The main research results and conclusions are as follows:

1. Producing large-diameter gears using gear rolling process with local induction heating is feasible.

2. The established FE model is validated by the comparison of simulation and experimental results of heating rates and rolling forces.
3. With local induction heating, the blank has a radial gradient temperature distribution, which results in the reduction of inner hole distortion. Owing to the heat compensation function, the defect of metal folding in the tooth top of the gear blank is reduced.
4. The formability of the blank is improved by the local induction heating method. Compared with cold rolling, the rolling force drops drastically using the local induction heating method.

Acknowledgements This work is supported by the National Natural Science Foundation of China (Grant No. 51375042) and China Postdoctoral Science Foundation (Grant No. 2015M580977).

References

1. Spotts MF (1978) Design of machine elements. Prentice-Hall, Englewood Cliffs, NJ, pp. 422–458
2. Dean TA (2000) The net-shape forming of gears. Mater Des 21: 271–278
3. Cai J, Dean TA, Hu ZM (2004) Alternative die designs in net-shape forging of gears. J Mater Process Technol 150:48–55
4. Choi JC, Choi Y (1999) Precision forging of spur gears with inside relief. Int J Mach Tools Manuf 39:1575–1588
5. Wang W, Zhao J, Zhai R, Ma R (2016) Variable contour two-step warm extrusion forming of spur gear and the deformation behavior of 20Cr2Ni4A steel. Int J Adv Manuf Technol:1–11. doi:10.1007/s00170-016-9027-0
6. Li Z, Wang B, Ma W, Yang L (2016) Comparison of ironing finishing and compressing finishing as post-forging for net-shape manufacturing. Int J Adv Manuf Technol:1–11. doi:10.1007/s00170-016-8424-8
7. Egan PF, Jones B, Connell G (1969) Production of gears by rolling. Proc Instn Mech Engrs 184:163–171
8. Kamouneh AA, Ni J, Stephenson D, Vriesen R (2007) Investigation of work hardening of flat-rolled helical-involute gears through grain-flow analysis, FE-modeling, and strain signature. Int J Mach Tools Manuf 47:1285–1291
9. Kamouneh AA, Ni J, Stephenson D, Vriesen R, DeGrace G (2007) Diagnosis of involutometric issues in flat rolling of external helical gears through the use of finite-element models. Int J Mach Tools Manuf 47:1257–1262
10. Neugebauer R, Klug D, Hellfritzsch U (2007) Description of the interactions during gear rolling as a basis for a method for the prognosis of the attainable quality parameters. Prod Eng Res Devel 1:253–257
11. Neugebauer R, Putz M, Hellfritzsch U (2007) Improved process design and quality for gear manufacturing with flat and round rolling. CIRP Ann Manuf Technol 56:307–312
12. Neugebauer R, Hellfritzsch U, Lahl M (2008) Advanced process limits by rolling of helical gears. Int J Mater Form 1:1183–1186
13. Zhang D, Zhao S (2014) New method for forming shaft having thread and spline by rolling with round dies. Int J Adv Manuf Technol 70:1455–1462
14. Zhang D, Zhao S, Wu S, Zhang Q, Fan S, Li J (2015) Phase characteristic between dies before rolling for thread and spline synchronous rolling process. Int J Adv Manuf Technol 81:513–528
15. Li J, Wang G, Wu T (2016) Numerical simulation and experimental study of slippage in gear rolling. J Mater Process Technol 234: 280–289
16. Lin Y, Chen X (2011) A critical review of experimental results and constitutive descriptions for metals and alloys in hot working. Mater Des 4(32):1733–1759
17. Ji H, Liu J, Wang B, Tang X, Huo Y, Zhou J, Hu Z (2016) Constitutive relationship of 4Cr9Si2 and technological parameters on the inner bore of cross wedge rolling for preform hollow valves. Int J Adv Manuf Technol 86:2621–2633
18. Skoczkowski TP, Kalus MF (1989) The mathematical model of induction heating of ferromagnetic pipes. IEEE Trans Magn 25: 2746–2747
19. Zhang D, Li Y, Fu J, Zheng Q (2009) Rolling force and rolling moment in spline cold rolling using slip-line field method. Chin J Mech Eng 22(5):688–695
20. Ji H, Liu J, Wang B, Zheng Z, Huang J, Hu Z (2015) Cross-wedge rolling of a 4Cr9Si2 hollow valve: explorative experiment and finite element simulation. Int J Adv Manuf Technol 77:15–26